Jurnal Tribologi 40 (2024) 199-211

MYTRIBOS Malaysian Tribology Society

Jurnal Tribologi

Website : jurnaltribologi.mytribos.org e-issn: 2289-7232

Investigations into friction, film thickness and heat generation of water-based lubricants containing nanoparticles, surfactant and dispersant in hydrodynamic journal bearing

M.A.H. Azizan, Nur Hidayatul Ezzaty Mohd Fadhli, Muhammad Adam Kamarudin, Muhammad Faris Idrus, Mohd Hafis Sulaiman *

Department of Mechanical and Manufacturing Engineering, Faculty of Engineering, Universiti Putra Malaysia, 43400 Serdang, Selangor, MALAYSIA.
*Corresponding author: hafissulaiman@upm.edu.my

KEYWORDS

Ceramic nanoparticle
Carbon nanoparticle
Water-based lubrication
Hydrodynamic journal bearing
Film thickness

ABSTRACT

Water-based lubrication offers superior cooling capacity compared to traditional oil-based lubrication. This study aims to evaluate the heat generation between sliding surfaces and the subsequent friction reduction using Water-based Lubricants (WBL) containing ceramic and carbon nanoparticles in hydrodynamic journal bearings. The nanoparticles used in this investigation include Magnesium Oxide (MgO), Silicon Carbide (SiC), a mixture of Magnesium Oxide and Silicon Carbide (MgO/SiC), Aluminium Oxide (Al_2O_3), and treated Graphene Oxide (tGO). The experiments were conducted on a TM 282 journal bearing test rig, with rotational speeds ranging from 200 to 1,200 rev/min, and under two different constant contact normal load settings of 10N and 15N. The methodology involved determining the minimum film thickness and constructing Stribeck's curve. The results demonstrate that heat generation remained low in all test WBLs due to the excellent cooling capacity of water, facilitating efficient heat dissipation and temperature reduction. Among the tested nanoparticles, tGO proved particularly effective in creating a complete separation between the rotating shaft and bearing surfaces, resulting in the highest film thickness and, consequently, a significant reduction in friction.

Received 27 September 2023; received in revised form 5 December 2023; accepted 22 January 2024.
To cite this article: Azizan et al., (2024). Investigations into friction, film thickness and heat generation of water-based lubricants containing nanoparticles, surfactant and dispersant in hydrodynamic journal bearing. Jurnal Tribologi 40, pp.199-211.

1.0 INTRODUCTION

Water-based lubricants (WBL) serve as a greener alternative to oil-based lubricants, using water as the base fluid with additives for specific applications. WBLs offer several advantages, including reduced toxic fume emissions that are harmful to the environment and easier cleaning, leading to lower maintenance costs, making them a more cost-efficient option (Rahman et al., 2021). The cooling properties of WBLs make them particularly suitable for applications where efficient cooling is essential. However, despite their lower cost compared to oil lubricants, WBLs may not be suitable for some tribological operations due to their corrosive nature (Tomala et al., 2010). Researchers are actively investigating the use of additives in WBLs to address this issue, as well as other tribological factors like friction and wear. Each type of additive serves a specific purpose when used with WBLs.

To overcome these limitations, various types of additives have been introduced to WBLs to enhance their tribological performance. These additives can be categorized based on their functions, including anti-wear (AW) agents, corrosion inhibitors, detergents, dispersants, extreme pressure (EP) additives, emulsifiers, and more. AW and EP additives are particularly crucial for WBLs due to their low viscosity, with nanoparticles such as TiO2 and Graphene Oxide (GO) nanosheets being notable examples (Rahman et al., 2021). Nanoparticles have the advantage of penetrating the microscopic gaps between surface asperities, leading to exceptional tribological properties (Loo et al., 2023). They achieve this through various mechanisms, including the rolling effect, mending effect, polishing effect, and the formation of a protective film. Nanoparticles rolling between surfaces transform sliding friction into rolling friction, reducing its magnitude. The mending effect involves nanoparticles filling in grooves or worn areas on the surface. Nanoparticles can also smoothen rough surfaces through the polishing effect, and by forming protective films through chemical reactions or tribo-sintering, they create a barrier between surfaces, preventing direct contact (Singh et al., 2019).

In rotating machines, the design of journal bearings, their dimensions, and clearance significantly influence their ability to mitigate vibrations caused by machine unbalance. A low clearance value increases the risk of surface contact due to reduced lubrication, while a higher clearance value is preferred to avoid this issue (Hirani et al., 2000). Besides accurate design values, operating variables, including the type of lubricant used, play a role in ensuring optimal performance under heavy loads. For instance, a study by Pierre and Fillon (2000) showed that ISO-VG 46 oil, thicker than ISO-VG 32, resulted in higher shaft temperatures at higher speeds in a plain journal bearing.

This study focuses on examining the lubricating effects of WBL containing various ceramic and carbon nanoparticles together with surfactant and dispersant in hydrodynamic journal bearing settings. The investigation includes evaluating friction reduction capabilities, heat generation, film thickness, and Stribeck's curve. Two different experimental parameter settings were considered: tests at increasing speeds and tests under constant contact normal loadings.

2.0 MATERIALS AND METHODOLOGY

In the preparation of the WBLs, deionized water served as the base fluid, while polyvinylpyrrolidone (PVP) as the surfactant and glycerol were used as dispersants. PVP acted as the surfactant to improve the dispersion stability of the lubricants. Glycerol, on the other hand, was added to enhance the viscosity of the lubricants, ultimately improving their load carrying capacity. The nanoparticles employed in this study included ceramic nanomaterials, ie. MgO, SiC,

a mixture of MgO/SiC, Al_2O_3, and carbon material, ie. tGO, all with a purity of 99% and particle sizes ranging from 20 to 40 nm. MgO and Al_2O_3 were obtained from Jiangsu XFNano Materials Tech Co., while SiC and graphene were supplied by Xi'an LY Health Technology Co. The specific concentration of nanoparticles applied is basically based on the optimal concentration obtained from other studies as shown in Table 1. This is because comparing the performance of lubricants with nanoparticles at the same concentration is meaningless, given that there exist optimal concentrations for achieving enhanced tribological performance among the tested lubricants. Such a comparison only identifies the best lubricants at specific concentrations, rather than pinpointing the overall best lubricant for the intended purpose.

As for the carbon nanoparticle, GO was employed because it has demonstrated exceptional tribological performance. GO possesses desirable properties such as easy shear capability, extreme strength and Young's modulus, high dispersibility in water, good conductivity, and high thermal stability (Xie et al., 2018). The initial attempt to prepare GO WBL using the existing GO resulted in poor dispersion stability. Therefore, to enhance the dispersion stability, treated Graphene Oxide (tGO) nanoparticles were prepared using a similar procedure as reported by Bautista-Flores et al. (Bautista-Flores et al., 2015). In the treatment procedure, graphene powder was mixed with 65-68% nitric acid at a ratio of 1:10 and stirred for 3 hours using an overhead stirrer. The resulting tGO dispersion was then neutralized with sodium hydroxide solution, filtered, and rinsed with deionized water to remove excess salts and chemicals. This process enhances the hydrophilicity of the existing graphene nanoparticles by decorating its surface with oxygen functional groups like hydroxyl and carboxyl groups, thus improving its dispersibility in WBL (Nyhilm et al., 2023).

The preparation of the water-based lubricants followed a two-step method, similar to a previous study by Zhou et al. (2022), as depicted in Figure 1 and summarized in Table 1. The concentration of nanoparticles were chosen at a specific concentration in order to achieve their optimal performances in improving the tribological performance (Goswami et al., 2020; Xie et al., 2018). This is a fundamental step since that there is an existence of optimal concentration for achieving improved tribological performance, hence comparing the performance of lubricants with constant nanoparticles additive concentration is incoherent (He et al., 2017; Singh et al., 2020; Y. Wang et al., 2017). Such a comparison only studies the best lubricants at specific concentrations, rather than focusing on the overall best lubricant for intended purposes. The process involved mixing DI water with glycerol using a magnetic stirrer, followed by gradual addition of PVP into the solution while stirring at 1,200 rpm. Subsequently, the ceramic-based nanoparticles were added and mixed using an overhead stirrer at the same speed for 30 minutes until no visible agglomerations were present in the lubricants. Any remaining agglomerations were then eliminated by subjecting the mixture to 120 W bath ultrasonication for an additional 30 minutes. In the case of SiC and SiC+MgO WBLs, the pH of the lubricants was adjusted to 10 using sodium hydroxide solution to improve its dispersion stability.

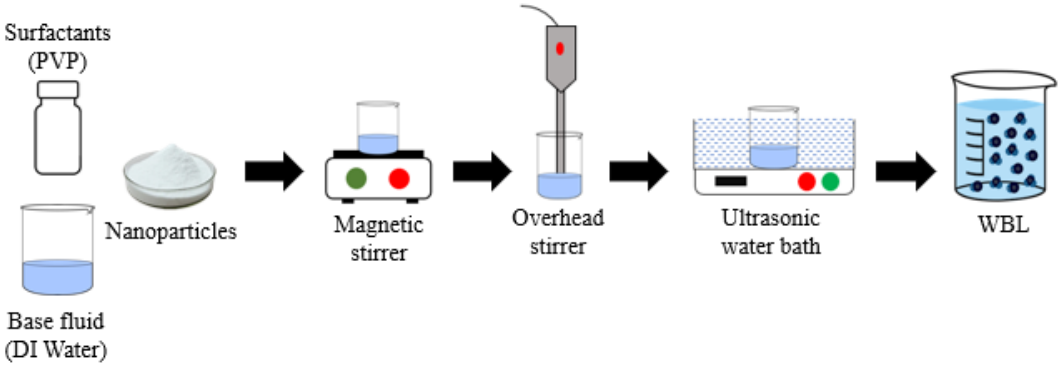

Figure 1: Preparation flow of the WBL containing nanoparticles, surfactant and dispersant. Adapted after Zhou et al., 2022.

Table 1: Formulations of the WBL containing surfactant, dispersant and different nanoparticles.

Test Lubricants	Content
MgO	0.3 wt% MgO nanoparticles + DI water + 2.0 wt% glycerol + 0.05 wt% PVP (Ahamed et al., 2020; Qamar et al., 2022)
SiC	0.3 wt% SiC nanoparticles + DI water + 2.0 wt% glycerol + 0.05 wt% PVP (Ahamed et al., 2020; Chen et al., 2017)
MgO/SiC	0.2 wt% MgO nanoparticles + 0.1 wt% SiC nanoparticles +DI water + 2.0 wt% glycerol + 0.05 wt% PVP (Zhang et al., 2016)
Al_2O_3	1.5 wt% Al_2O_3 nanoparticles + DI water + 2.0 wt% glycerol + 1.0 wt% PVP (J. Wang et al., 2021)
tGO	0.5 wt% tGO nanoparticles + DI water + 2.0 wt% glycerol + 0.1 wt% PVP (Gao et al., 2019; Keklikcioglu Cakmak, 2020)

*Note: The nanoparticle concentrations were selected based on optimal concentration obtained from other studies as mentioned above.

Figure 2 shows the experimental setup using the hydrodynamic journal bearing setting. To conduct the experiment, the drip oiler (2) was filled with the test WBL, which delivered the lubricant into the bearing housing. An intrinsic weight of 10 N and a load of 15 N were set on the platform (3), connected to a lever and pulley that exerted a load on the journal bearing. Then, the sliding weight (4) was moved to the far left before the motor was turned on. The speed was set to 200 rev/min, and the sliding weight was adjusted until it achieved balance. The distance taken to balance, *a* (mm), was recorded for each speed increment of 200 rev/min. Each test session ended when the weight balanced during the final speed setting 1000 rev/min.

After each test, the drip oiler was uninstalled using a set of Allen keys, and each component was thoroughly wiped with tissue paper containing acetone. Next, the clear cover of the journal bearing housing was also uninstalled to enable cleaning of the journal bearing and the lubricating grooves. Once the surfaces dried, the clear cover was reinstalled, and the drip oiler was reattached to the test rig. The next test WBL was poured, and testing could begin.

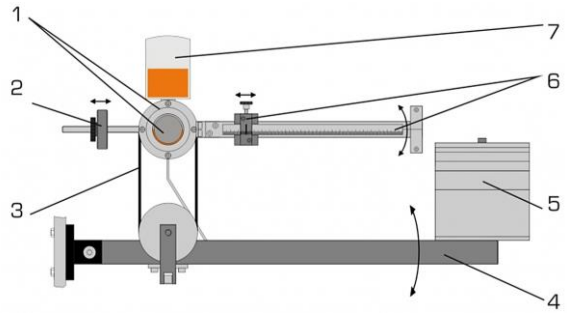

Operating conditions:

Parameters	Values
Normal load	10 N and 15 N
Temperature	30 °C
Speed	200 – 1,200 rev/min
Speed increment	200 rev/min

Figure 2: Schematic of the hydrodynamic journal bearing test apparatus. Adapted after G.U.N.T. Hamburg, 2023. [1] journal bearing housing with shaft journal, [2] tare weight, [3] belt to transfer force to the bearing housing, [4] loading lever, [5] weights, [6] measuring lever with scale and sliding weight, [7] drip oiler.

To assess the performance of each lubricant and construct Stribeck's curve for facilitating the discussion, certain essential values need to be calculated. This section presents the equations employed to determine the following parameters:

Moment of friction M_{fric};

$$M_{fric} = F \cdot a \tag{1}$$

where F = sliding weight mass, N, and a = sliding weight distance, mm

Frictional force F_{fric};

$$F_{fric} = \frac{M_{fric}}{r} \tag{2}$$

where r = journal radius, 15 mm.

Coefficient of friction μ;

$$\mu = \frac{F_{fric}}{F_{sum}} \tag{3}$$

where $F_{sum} = F_{intrin} + 5 \cdot F_{load}$ and $F_{intrin} = 5N$ (G.U.N.T. Hamburg, 2023).

Minimum film thickness h_{min} was calculated based on the Hamrock and Dowson model (Hamrock et al., 2004):

$$h_{min} = 2.8R\left(\frac{\eta V}{E * R}\right)^{0.65}\left(\frac{F}{E * R^2}\right)^{-0.21} \tag{4}$$

where η is dynamic viscosity, Pa.s, V is speed, m/s, E^* is Effective Young's modulus, Pa.

Finally, the Stribeck's curve was determined using the Hersey Number H_N, which is calculated using the following formula:

$$H_N = \frac{\eta V}{F_N} \tag{5}$$

where F_N is normal force, N.

3.0 RESULTS AND DISCUSSION

Figure 3 illustrates the trends of the moment of friction for all tested WBLs when the journal bearing was operated at various speeds in the range of 200 rpm to 1,200 rpm under a constant normal load of 15 N. For all WBLs, the increment of frictional speed contributed to rapid falls, approaching an infinite value of frictional moment. At a speed of 200 rpm, Al_2O_3 recorded the highest moment of friction, while the lowest water-based lubricant, MgO, was at the bottom point of the curve with a value of 61 Nm. Thus, it can be concluded that the bearing and rotational shaft exhibited higher frictional characteristics when operated under Al_2O_3 additive compared to the MgO additive at low speed. However, the frictional moment of Al_2O_3 underwent a gradual drop, indicating its effectiveness as a lubricant in reducing friction with an increase in rotational speed. Similar situations applied to the MgO, a mixture of MgO/SiC, SiC, and tGO additives, as friction reached a steady-state level when the speed was increased.

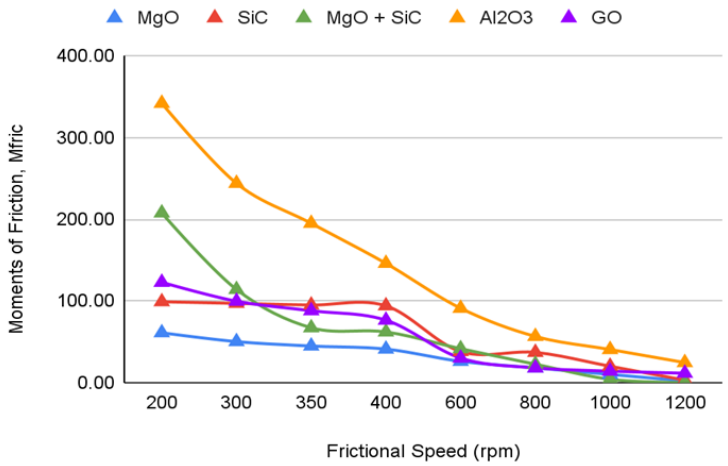

Figure 3: Moment of friction, M_{fric} as a function of rotational speed.

The temperature variation of all five tested WBL is presented in the scatter graph in Figure 4. For all lubricants (except SiC), the temperature range remained mostly at 34°C, with a slight increase in temperature values (e.g., Al_2O_3). The temperature variation reflects the heat generation resulting from friction between the bearings and the lubricant. These temperatures were consistently maintained, even with increments in the shaft speed, to ensure effective heat dissipation and promote stable operating conditions. It was essential to control these temperatures to prevent heat accumulation from exceeding the bearing temperature, which could potentially impact the bearing performance and lead to damage or failure. This situation also applied to the temperature variation of tGO at different loads of 15 N and 10 N (as shown in Figure 5).

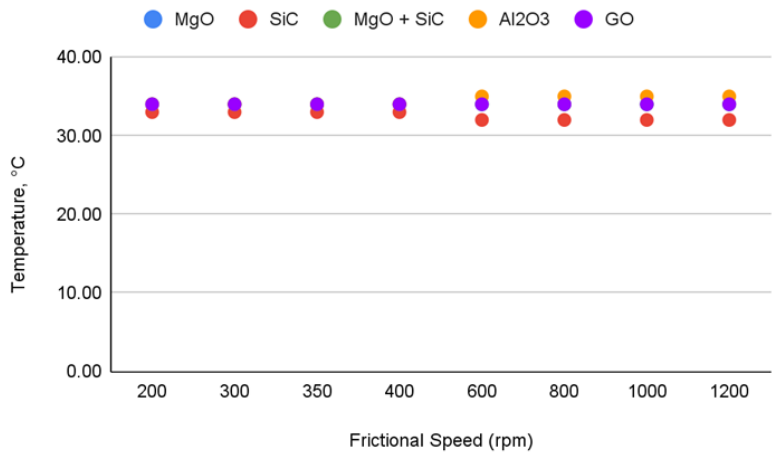

Figure 4: Temperature vs. Speed of all five tested water-based lubricant.

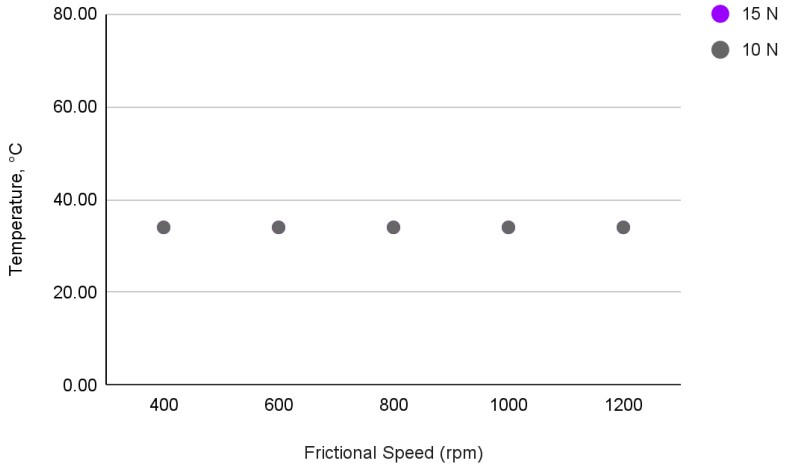

Figure 5: Temperature vs. speed of graphene oxide at 15 N and 10 N.

The Stribeck's curve, comprising the coefficient of friction against the Hersey number, was a crucial tool for understanding how the WBLs behaved under various operating conditions. In this study, it is realized that the performance of the WBLs could be influenced by the types of test nanoparticles in WBLs, which was quantified by the Hersey number. Figure 6 presented the Stribeck's curve for five different nanoparticles that acted as nanoadditives in WBLs, namely MgO, SiC, MgO/SiC, Al_2O_3, and tGO, as well as the Stribeck's curve for different loads for the tGO additive.

In the case of the MgO nanoadditive under a constant 15 N load, the Stribeck's curve appeared almost linear, with a Hersey number of 0.23 at a coefficient of friction of 0.051 at low speed. The curve continued to decline until it reached a Hersey number of 1.13, with a coefficient of friction of 0.008. This trend indicated that as the Hersey number increased, the coefficient of friction decreased, resulting in lower resistance for the lubricant to flow. The Hersey number's relationship with the viscosity and speed of the lubricant explained this behavior. According to Akbarzadeh & Khonsari (2009), the reduction in friction coefficient was due to an increase in the fluid film's thickness and a corresponding decline in the role of asperities in load transportation.

The friction coefficient continued to decrease until the lubrication regime shifted from mixed to full elastohydrodynamic lubrication, where the entire load was carried by the fluid film.

For the SiC nanoadditive under the same load, the coefficient of friction remained almost constant until it reached a Hersey number of 2.40, after which it decreased significantly until reaching a Hersey number of 3.60. Subsequently, it decreased gradually until reaching a Hersey number of 6.00. On the other hand, the Stribeck's curves of MgO/SiC and Al_2O_3 exhibited nearly similar linear curves as MgO under different conditions, owing to the different viscosities of these lubricants. As for the Stribeck's curve of tGO, an increase in the Hersey number led to a rapid decrease in the coefficient of friction, creating a steep curve until reaching a certain point before it continued to decrease steadily. The same trend was observed in the Stribeck's curve of tGO under a 10 N load, which exhibited a similar pattern to the Stribeck's curve of tGO under a 15 N load.

It has been found out that each Stribeck's curve of MgO, SiC, MgO/SiC, Al_2O_3, and tGO displayed its unique trend and pattern, with some curves being linear while others fluctuated. However, the common trend was that as the Hersey number increased, the coefficient of friction decreased. Lastly, the comparison between the same lubricant under different loads revealed that although the curve's pattern remained the same, the lower the load, the steeper the curve and the more rapidly it increased.

Using tGO nanoparticle in the WBL, the influence of contact loadings on water lubrication was studied. Figure 7 shows the measured friction corresponding to the different speeds under a constant contact normal loadings 10 N and 15 N. At 600 rpm, both curves indicated that the frictional value was dominated by graphene oxide with a load of 10 N compared to a load of 15 N. This finding suggested that friction between the bearings and the lubricant was higher at a load of 10 N than at a load of 15 N on the platform. At 600 rpm, for a load of 10 N, the resistive force between the bearings and lubricant gradually dropped, reaching a lower value than that of 15 N loads (for both curves). This occurred because under low loading conditions (with a low magnitude of applied load), the pressure distribution in the lubrication film at the bearing was also low. Consequently, the deformation potential of the lubrication film reduced, leading to an increase in the separation between lubrication film gaps (Vladescu et al., 2018). As a result, the contact between the journal and bearing was minimized, leading to reduced frictional forces as the journal speed increased to higher velocities, up to 1,200 rpm.

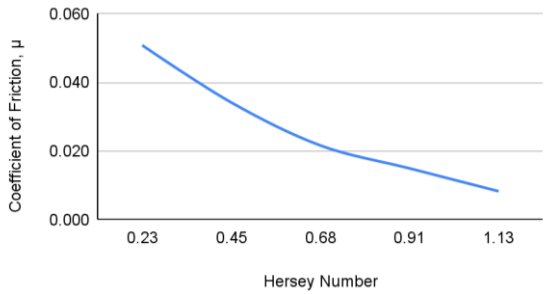

Stribeck's curve of MgO (at 15 N load)

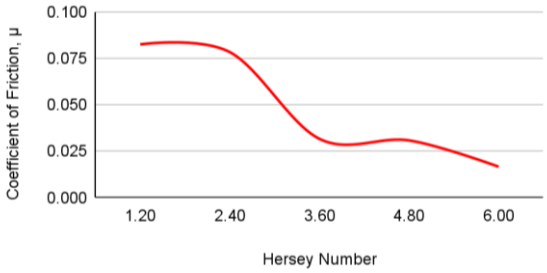

Stribeck's curve of SiC (at 15 N load)

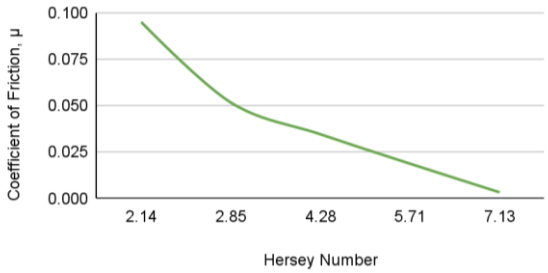

Stribeck's curve of MgO/SiC (at 15 N load)

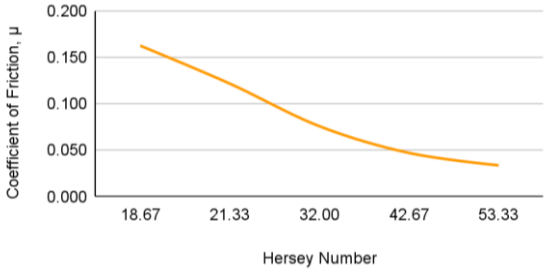

Stribeck's curve of Al_2O_3 (at 15 N load)

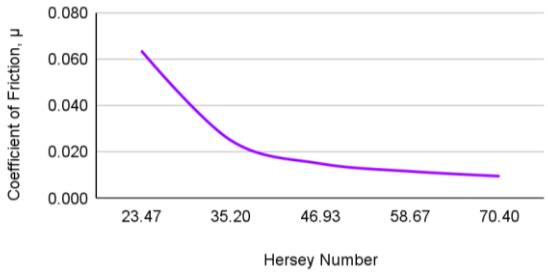

Stribeck's curve of tGO (at 15 N load)

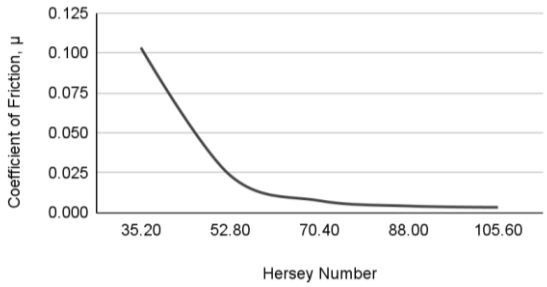

Stribeck's curve of tGO (at 10 N load)

Figure 6: Stribeck's curve of all five tested WBLs containing different nanoparticles.

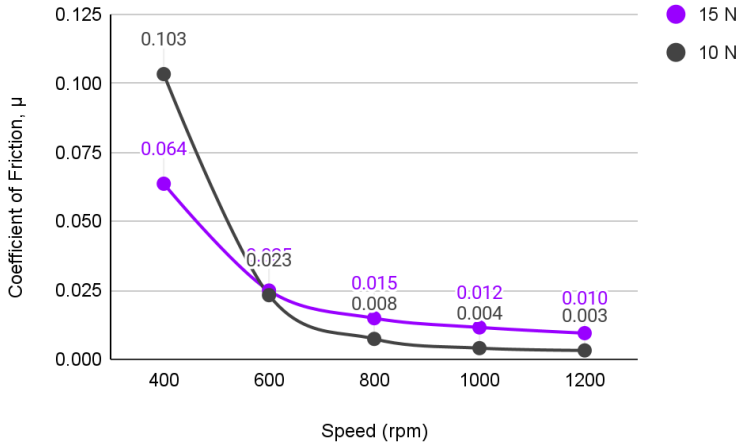

Figure 7: Friction coefficient with respect to speed for tGO WBL at constant load 10N and 15N.

Table 2 illustrates the comparison of the minimum film thickness of the tested WBLs, as observed from their Stribeck's curves, which varied considerably. The minimum film thickness in hydrodynamic journal bearings refers to the smallest distance between the rotating shaft and the bearing surface where a lubricating film is present. It represents the thinnest portion of the fluid film that separates the two surfaces. In this case, the evaluation of the lubricating film was done using Equation 4 from the Hamrock and Dowson model. The film thickness was measured at a speed of 1,000 rpm for each nanoparticle type.

From Table 2, it can be observed that tGO and Al_2O_3 nanoadditives had a higher minimum film thickness compared to the other additives. A greater h_{min} value in both tGO and Al_2O_3 ensured that there was sufficient separation between the two surfaces during operation, preventing direct metal-to-metal contact and providing load-bearing capability (Sun & Changlin, 2004). Consequently, a thicker lubricating film resulted in lower friction as there was less interaction between the surfaces.

Additionally, for the tGO WBL, a comparison of film thickness was made by changing the load of the weight platform from 15 N to 10 N. According to Table 2, it appeared that the tGO WBL with a load of 10 N had a larger and thicker film with a value of 2.623 μm compared to the lubricating film operating with a load of 15 N. Under high loading conditions, the pressure distribution exerted on the bearings increased, and this pressure might compress the lubricating film, causing a reduction in lubricating thickness (Nikolakopoulos & Papadopoulos, 2008). Consequently, frictional forces exerted would be higher, leading to temperature elevation. As a result, the lubricant tended to lose its viscosity and thin out, thereby reducing the effectiveness of the lubricating film.

Table 2: Calculated minimum film thickness for the test WBLs.

Type of nanoparticles	Load (N)	Minimum film thickness, h_{min} (μm)
MgO	15	0.185
SiC	15	0.547
MgO/SiC	15	0.612
AL_2O_3	15	2.264
tGO	15	2.409
tGO	10	2.623

CONCLUSIONS

In this study, the hydrodynamic journal bearing was utilized to examine the lubricating capabilities of MgO, SiC, hybrid MgO/SiC, Al_2O_3, and tGO nanoparticles as nanoadditives together with surfactant and dispersant in WBLs. The load was maintained at 15 N throughout all test sessions, while the WBLs were changed after each test. Meanwhile, one test with tGO WBL was run at 10 N to test the effect of contact loading on friction properties. The journal speed had an initial speed of 200 rpm with an increment of 200 rpm for four consecutive tests. Based on the results obtained from the experiments, the following conclusions can be drawn:

a) All WBLs were able to operate at a stable temperature of 33.83°C on average, despite the speed increments.
b) Al_2O_3 was the least desirable WBL as it had the highest coefficient of friction at all speed variations.
c) The best performing WBL was tGO as it had the highest separation between the journal and bearing surfaces, reducing the amount of friction during operation.
d) The coefficient of friction for tGO began to decrease steadily after 600 rpm and produced a similar curve for both loads.
e) SiC produced an almost ideal Stribeck's curve, where all regions of the curve were present, but the hydrodynamic region peaked at 800 rpm before decreasing gradually.
f) It is suggested to investigate the effect of loads with a larger variety on MgO and tGO to study their load-bearing capabilities.

ACKNOWLEDGEMENTS

The authors would like to declare that this study and publication were supported by the Ministry of Higher Education under Fundamental Research Grant Scheme (FRGS/1/2022/TK10/UPM/02/9) and the Universiti Putra Malaysia GP-IPM (UPM/GP-IPM/2022/9717500). The authors would like to extend their gratitude to the Department of Mechanical and Manufacturing Engineering, Faculty of Engineering, Universiti Putra Malaysia for their assistance and for making their facilities available at every stage of this research.

REFERENCES

Ahamed, M. M., Basha, S. M. J., & Prasad, B. D. (2020). Comparison of Thermo-Physical and Tribological Characteristics of Nanolubricant. In L. Vijayaraghavan, K. H. Reddy, & S. M. Jameel Basha (Eds.), Emerging Trends in Mechanical Engineering (pp. 153–164). Springer Singapore.

Akbarzadeh, S., & Khonsari, M. M. (2009, December 5). Effect of Surface Pattern on Stribeck Curve. Tribology Letters, 37(2), 477–486. https://doi.org/10.1007/s11249-009-9543-2.

Bautista-Flores, C., Sato-Berrú, R. Y., & Mendoza, D. (2015). Doping graphene by chemical treatments using acid and basic substances. Journal of Materials Science and Chemical Engineering, 3(10), 17. https://doi.org/10.4236/msce.2015.310003.

Chen, W., Zou, C., Li, X., & Li, L. (2017). Experimental investigation of SiC nanofluids for solar distillation system: Stability, optical properties and thermal conductivity with saline water-based fluid. International Journal of Heat and Mass Transfer, 107, 264–270. https://doi.org/10.1016/j.ijheatmasstransfer.2016.11.048

G.U.N.T. Hamburg. (2023). TM 282 Journal Bearing Friction Apparatus. Retrieved from https://www.gunt.de/en/products/040.28200/tm282 /

Gao, H., Hu, G., & Liu, H. (2019). Preparation of a Highly Stable Dispersion of Graphene in Water with the Aid of Graphene Oxide [Research-article]. Industrial and Engineering Chemistry Research, 58(38), 17842–17849. https://doi.org/10.1021/acs.iecr.9b03771

Goswami, R., Verma, S., & Das, R. (2020). Energy Production Through Gasification of Waste Biomass in Punjab Region. In Lecture Notes in Mechanical Engineering. https://doi.org/10.1007/978-981-32-9931-3_51

Hamrock, B. J., Schmid, S. R., & Jacobson, B. O. (2004). Fundamentals of Fluid Film Lubrication. CRC Press

He, A., Huang, S., Yun, J. H., Wu, H., Jiang, Z., Stokes, J., Jiao, S., Wang, L., & Huang, H. (2017). Tribological Performance and Lubrication Mechanism of Alumina Nanoparticle Water-Based Suspensions in Ball-on-Three-Plate Testing. Tribology Letters, 65(2). https://doi.org/10.1007/s11249-017-0823-y

Hirani, H., Athre, K., & Biswas, S. (2000). Comprehensive design methodology for an engine journal bearing. Proceedings of the Institution of Mechanical Engineers, Part J: Journal of Engineering Tribology, 214(4), 401–412. https://doi.org/10.1243/1350650001543287.

Keklikcioglu Cakmak, N. (2020). The impact of surfactants on the stability and thermal conductivity of graphene oxide de-ionized water nanofluids. Journal of Thermal Analysis and Calorimetry, 139(3), 1895–1902. https://doi.org/10.1007/s10973-019-09096-6

Loo DL, Teoh YH, How HG, Le TD, Nguyen HT, Rashid T, et al. Effect of nanoparticles additives on tribological behaviour of advanced biofuels. Fuel 2023;334:126798. https://doi.org/10.1016/j.fuel.2022.126798.

Nikolakopoulos, P. G., & Papadopoulos, C. (2008). A study of friction in worn misaligned journal bearings under severe hydrodynamic lubrication. Tribology International, 41(6), 461–472. https://doi.org/10.1016/j.triboint.2007.10.005

Nyholm, N., & Espallargas, N. (2023). Functionalized carbon nanostructures as lubricant additives–A review. Carbon, 201, 1200-1228. https://doi.org/10.1016/j.carbon.2022.10.035.

Pierre, I., & Fillon, M. (2000). Influence of geometric parameters and operating conditions on the thermohydrodynamic behaviour of plain journal bearings. Proceedings of the Institution of Mechanical Engineers, Part J: Journal of Engineering Tribology, 214(5), 445-457. https://doi.org/10.1243/1350650001543322.

Qamar, A., Anwar, Z., Ali, H., Shaukat, R., Imran, S., Arshad, A., Ali, H. M., & Korakianitis, T. (2022). Preparation and dispersion stability of aqueous metal oxide nanofluids for potential heat transfer applications: a review of experimental studies. Journal of Thermal Analysis and Calorimetry, 147(1), 23–46. https://doi.org/10.1007/s10973-020-10372-z

Rahman MH, Warneke H, Webbert H, Rodriguez J, Austin E, Tokunaga K, et al. Water-based lubricants: Development, properties, and performances. Lubricants 2021;9. https://doi.org/10.3390/lubricants9080073.

Singh A, Chauhan P, Mamatha TG. A review on tribological performance of lubricants with nanoparticles additives. Mater Today Proc, vol. 25, Elsevier Ltd; 2019, p. 586–91. https://doi.org/10.1016/j.matpr.2019.07.245.

Singh, Y., Sharma, A., Singh, N. K., & Noor, M. M. (2020). Effect of SiC nanoparticles concentration on novel feedstock Moringa Oleifera chemically treated with neopentylglycol and their trobological behavior. Fuel, 280(July), 118630. https://doi.org/10.1016/j.fuel.2020.118630

Sun, J., & Chang-Lin, G. (2004). Hydrodynamic lubrication analysis of journal bearing considering misalignment caused by shaft deformation. Tribology International, 37(10), 841–848. https://doi.org/10.1016/j.triboint.2004.05.007

Tomala, A., Karpinska, A., Werner, W. S. M., Olver, A. V., & Störi, H. (2010). Tribological properties of additives for water-based lubricants. Wear, 269(11–12), 804–810. https://doi.org/10.1016/j.wear.2010.08.008.

Vladescu, S., Marx, N., Fernández, L. C. M., Barceló, F., & Spikes, H. (2018). Hydrodynamic Friction of Viscosity-Modified Oils in a Journal Bearing Machine. Tribology Letters, 66(4). https://doi.org/10.1007/s11249-018-1080-4

Wang, J., Hu, W., & Li, J. (2021). Lubrication and anti-rust properties of jeffamine-triazole derivative as water-based lubricant additive. Coatings, 11(6). https://doi.org/10.3390/coatings11060679

Wang, Y., Li, C., Zhang, Y., Yang, M., Zhang, X., Zhang, N., & Dai, J. (2017). Experimental evaluation on tribological performance of the wheel/workpiece interface in minimum quantity lubrication grinding with different concentrations of Al2O3 nanofluids. Journal of Cleaner Production, 142, 3571–3583. https://doi.org/10.1016/j.jclepro.2016.10.110

Xie, H., Jiang, B., Dai, J., Peng, C., Li, C., Li, Q., & Pan, F. (2018). Tribological behaviors of graphene and graphene oxide as water-based lubricant additives for magnesium alloy/steel contacts. Materials, 11(2), 206. https://doi.org/10.3390/ma11020206.

Zhang, X., Li, C., Zhang, Y., Jia, D., Li, B., Wang, Y., Yang, M., Hou, Y., & Zhang, X. (2016). Performances of Al2O3/SiC hybrid nanofluids in minimum-quantity lubrication grinding. International Journal of Advanced Manufacturing Technology, 86(9–12), 3427–3441. https://doi.org/10.1007/s00170-016-8453-3